Multi-objective Optimization of Solar Thermal Systems Applied to Residential Building in Portugal

Ana Cristina Ferreira[1,2(✉)], Ângela Silva[1,3,4], and Senhorinha Teixeira[1]

[1] ALGORITMI Centre, University of Minho, Guimarães, Portugal
acferreira@dps.uminho.pt
[2] Mechanical Engineering and Resource Sustainability Center (MEtRICs), University of Minho, Guimarães, Portugal
[3] Centro de Investigação em Organizações, Mercados e Gestão Industrial (COMEGI), Universidade Lusíada Norte, Vila Nova de Famalicão, Portugal
[4] Escola Superior de Ciências Empresariais, Instituto Politécnico de Viana do Castelo, Valença, Portugal

Abstract. Thermal-economic evaluation represents an effective tool to optimize thermal systems. This study presents a mathematical model that encloses the physical variable equations and a set of equations that define the purchase cost of the main system components. The main objective of this study is the thermo-economic optimisation of solar thermal systems for residential building applications, considering a multi-objective approach. The simulations were performed through a MatLab code, by implementing an elitist variant of NASGA-II. The numerical model disclosed a Pareto front considering the optimal trade-off solutions for the minimum investment cost and the maximum solar collection efficiency. The optimal solutions disclose a set of optimal solutions for which the solar collection efficiency vary 28.3% and 77.0% and the investment costs vary between 2,099€ and 3,308€. Results show that gains in solar collection efficiency above 70% imply a great increase in the total purchase cost, implying a bump of almost 1,000€, from a total investment cost of 2,200€ to 3,200€. As a conclusion, the solar collector area is one of the most important decision variables in the multi-objective optimization of thermal-economic analysis of solar thermal systems.

Keywords: Solar thermal systems · Multi-objective optimisation · NSGA-II

1 Introduction

All over the world, the implementation of solar thermal systems to suppress the domestic hot water needs has been increasing over the years, mostly, as a way to increase the energy efficiency in the residential sector [1]. The greatest advantage of solar energy is that it is clean and can be supplied without any environmental pollution. However, the proper sizing of the components of a solar energy system is a complex

© Springer Nature Switzerland AG 2019
S. Misra et al. (Eds.): ICCSA 2019, LNCS 11624, pp. 26–39, 2019.
https://doi.org/10.1007/978-3-030-24311-1_2

problem, which includes both predictable (collector and other components' performance characteristics) and unpredictable (weather) data [2].

Important factors that affect the solar heat market are the costs of the plant components, the characteristics of the infrastructures and the local conditions regarding the solar irradiation and the energy consumption. In fact, and despite all the technological considerations, the cost of a solar-thermal system may vary by up to 20% from the average, depending on the collector design and building exposure to the sunlight. Solar collectors typically supply 60% to 80% of the hot water needs, whereas the remaining 20–40% is provided by another heat source, usually electricity or gas [3]. Kalogirou presented a review referring several types of solar thermal collectors and applications, such as flat-plate, parabolic trough, evacuated tube, Fresnel lens, parabolic dish and helio stat field collectors which are used in this system [4]. The solar collectors can be used for domestic, commercial and industrial purposes. Ong and Tong present in their study a system composed of solar water heaters depending upon collector and storage tank design and sizing and weather conditions (solar radiation intensity and ambient temperature) [5].

In recent years, studying the optimum performance of energy systems with thermodynamic models have been an attractive option for researchers [5–9]. Ust, Sahin and Kodal [6] introduced a new thermo-economic performance analysis based on an objective function defined as the power output per unit of total cost. It is of utmost importance to integrate costs and physical variables to simultaneously optimize the economic and physical output. Thermal-economics combines thermodynamic analysis and economic principles to evaluate the costs of energy production in each of the power plant components [7, 8]. These costs can be useful to disclose the most cost-effective configuration of the components and, then, improving the overall system design the components and, then, improving the overall system design [9]. Assaf and Shabani [10] developed a sizing multi-objective optimisation using the genetic algorithm on a solar-hydrogen combined heat and power system integrated with solar-thermal collectors to supply both power and heat (i.e. hot water demand) to an application. Lin et al. [11] also presented a multi-objective optimisation strategy for thermal energy storage using phase change materials for solar air systems, in which two performance indicators of average heat transfer effectiveness and effective phase change materials charging time were used as the conflicting objectives. In [12], a building integrated solar thermal system with seasonal storage was optimized with the use of TRNSYS modelling software in order to evaluate different integration options of the solar collector array. The model calculates the space heating needs during the heating period as well as the annual domestic hot-water needs of a typical single-family detached home in the city of Thessaloniki. More recently, Yılmaz [13], proposed a novel methodology for determining the optimum orientation and sizing of water-in-glass evacuated tube solar water heating systems, for residential usage. A transient model was conducted for the prediction of a full year's system performance via the System Advisor Model. Asadi *et al.* [14] presented a combination of thermo-economic analysis and multi-objective optimization of a 10 kW single-effect ammonia-water solar absorption cooling system. A thermodynamic model is derived, and energy-exergy analyses are conducted. Also, the effects of various solar collector types including a flat plate, evacuated tube, compound parabolic, and parabolic trough collectors on the system performance are examined at different ambient temperatures.

The studies available in the literature are mostly focused in the analysis of either a solar thermal system with a single fixed technology where the goal is to optimise a single component and its operational conditions or find the best option and size for a specific application [5, 10–12, 15]. The purpose of the present work is distinct from those perspectives: the main objective is the development of a simplified optimisation model that reveals the optimal values for the physical variables (e.g. solar collector area, storage tank volume) that will lead to lowest investment cost without compromising the solar collection efficiency. A set of equations, modelling the thermodynamics of a solar thermal system, was defined to calculate the physical system variables. Based on a costing methodology, the investment cost equations for the thermal system are also defined. Each cost equation is formulated considering the most relevant physical parameter that influences the cost of a certain component. The numerical solution was obtained using NSGA-II, through MatLab® software. A Pareto front was determined, disclosing the best solutions considering the investment cost minimization and the maximization of solar collection efficiency as objective functions.

2 System Description and Physical Model

2.1 System Description

The solar radiation is converted directly into thermal energy and it is absorbed and transferred to a fluid stream. Most commercial and domestic applications are built-in at low and medium-temperature ranges (40 °C to 80 °C), which in fact corresponds to the largest share of heat consumption, mainly Domestic Hot Water (DHW) and space heating [3, 4]. The most important components of a solar thermal system are the solar collector, the pump and a controller (in the case of active systems), the storage tank to accumulate heat from the working fluid and the circuit of pipes (see the representative scheme at Fig. 1). These are the most important components when sizing solar thermal systems considering energy production and storage.

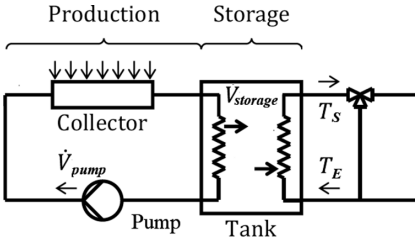

Fig. 1. Scheme of the main circuit of the solar thermal system.

The solar collector is the main component of solar thermal systems. The sunlight is absorbed by a material, converted to heat and transferred to a fluid stream. The heated fluid (generally air, water, or antifreeze liquid) can be used for several purposes such as space heating, hot-water heating, process heating, and even cooling.

Several designs of flat solar collectors are available, including with or without single or multiple glass covers, or with a vacuum for reducing the heat losses in so-called unglazed, glazed or evacuated collector designs, respectively. The presence of a glass layer or vacuum allows operation with higher efficiencies at higher temperatures over an extended temperature range. For domestic use, the temperature at the point of supply is, usually, of about 45 °C. To reach that temperature, the heated water temperature should be accumulated at a temperature of 60 °C.

2.2 Mathematical Modelling

The useful power collected by the thermal fluid (see Eq. (1)), can be estimated by the correlation between the solar collection area (A_{solar}), solar irradiation (I_g), collector absorbance (α), collector aperture transmittance (τ), the global losses coefficient (U_L) and the temperature variation between the mean temperature of the thermal fluid (15 °C $\leq t_f \leq$ 180 °C) and the ambient temperature (assumed to be a fixed temperature, t_a = 15 °C). When using directly the mean temperature of the fluid, it is necessary to introduce a corrector factor, the irrigation factor, F', which reduces the useful power and takes the value of 0.789.

$$P = A_{solar} \cdot F' \cdot \left[I_g \cdot \tau \cdot \alpha - U_L \left(t_f - t_a \right) \right] \tag{1}$$

The solar collection efficiency is defined by the ratio between the captured and the received energy. The efficiency of the collection ($\eta_{collection}$) of the solar collection might be calculated as the Eq. (2) for a certain mass flow of thermal fluid.

$$\eta_{collection} = F'(\tau\alpha) - (F'U_L)\, T^* - (F'U_L)\, I_g\, T^{*2} \tag{2}$$

The linear losses coefficient $F'U_L$ was assumed to be 3.6844 W/m^2 K. The term T^* represents the maximum temperature that the collector can reach for certain ambient temperature and solar irradiation, as defined as in Eq. (3).

$$T^* = \frac{\left(t_f - t_a \right)}{I_g} \tag{3}$$

Based on the data from several commercial models, the solar collection efficiency can be approximated to a second-degree polynomial function as presented in Fig. 2.

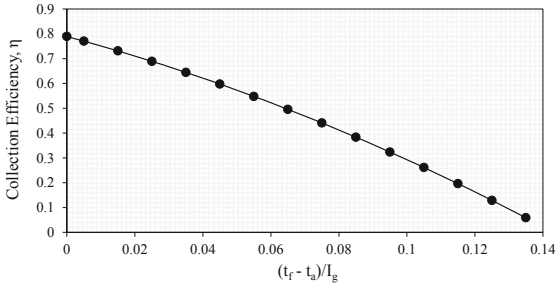

Fig. 2. Characteristic curve of solar collection efficiency, as a function of the maximum temperature that the collector can reach for certain ambient temperature and irradiation.

When solar energy is enough to increase the thermal fluid temperature and the heat transfer process is ensured, water circulates from storage to the collector. Then, the heated water returns to the storage tank, where it is stored until it is needed. As a pump circulates the water, the collectors can be mounted either above or below the storage tank.

Direct circulation systems often use a single storage tank equipped with an auxiliary water heater, but two-tank storage systems can also be used [4, 15]. The mass flow that is pumped in the primary circuit depends on the collection aperture area and the thermal properties of the thermal fluid that is used in the system, the specific heat (c_p) and the density (ρ_{tfluid}), as presented in the Eq. (4). The thermal fluid used in the primary circuit is a mixture of antifreeze with water in appropriate concentrations to the minimum temperature of a certain location.

$$\dot{V}_{pump} = \left(\frac{10F'U_{L0}}{c_{p\ tfluid}} \cdot A_{solar} \cdot 3600 \right) \cdot \frac{1}{\rho_{tfluid}} \tag{4}$$

The need for energy does not always coincide with the time of production, so it is necessary to have an accumulation system to meet the demand in times of low radiation or no consumption. The use of vertical tanks has the advantage of favouring water stratification. Thus, it is ensured that the hottest water is in the upper part of the accumulator, which is precisely where it is extracted. There is a correlation between the percentage of incident solar energy use and the optimum volume of the deposit per unit area of the solar collector, as presented by the Eq. (5). According to [16], the optimal storage volume per unit of solar collection area is 0.070 m^3/m^2. Higher values do not lead to greater use of incident solar energy, but only contribute to the increase in the storage tank volume and its cost [16].

$$0.060\,\mathrm{m}^3/\mathrm{m}^2 < \frac{V_{storage}}{A_{solar}} < 0.090\,\mathrm{m}^3/\mathrm{m}^2 \tag{5}$$

2.3 Energy Requirements to Suppress DHW of a Reference Building

Considering a residential building, located in Lisbon, with an occupation of 4 people with a need of 40 L of water per person and per day at 60 °C, the daily hot water consumption correspond to 160 L day^{-1}. The solar panel is optimally oriented, 45° South, and set with an inclination of 51° angle [17].

The specific daily hot water consumption was calculated by taking into account the ratio between the water need per person, per day, divided by the number of residents. Table 1 gives a summary of all input parameters to calculate the thermal requirements for DHW. The energy required to suppress the DHW needs (Q_{DHW}) can be calculated by the Eq. (6), where ΔT is the temperature increase from the grid water temperature, which was assumed to be 35 °C.

$$Q_{DHW} = Cons_{dhw} \cdot (4.187/3600) \cdot \Delta T \cdot 365\,days \tag{6}$$

Table 1 Input parameters to calculate the thermal requirements for DHW

Parameter	Value
Daily hot water consumption, C_{onsDHW}	160 L day^{-1}
Hot water temperature	60 °C
Panel direction	South (45°)
Yearly sum of global irradiation (Lisbon)	1,890 kWh/m^2
Q_{DHW}	**2,377 kWh.year^{-1}**

For this reference scenario, the energy required to suppress the DHW needs is approximately 2 377 kWh year^{-1}. According to [16], at least, an equivalent area of 1 m^2 of solar collection is required to suppress a demand of 500 kWh year^{-1}.

3 Economic Model of Solar Thermal Components

The costing methodology, based on the approach developed by [18], consists on the derivation of a cost expression for each component by integrating thermodynamic and cost coefficients, adjusted for this kind of technology, and also taking into account real market data. Each cost equation was defined considering physical variables, which can be classified as size and quality variables. In terms of methodology, the equations are defined considering that the cost of each component is based on a reference case and includes a cost coefficient, a reference size factor, F_{ref}, which scales the component and, for some system components, a quality factor. The basic formulation is presented in the Eq. (7):

$$\mathrm{C_i} = C_{ref,i}\, F_{ref} \cdot \left(\frac{F_i}{F_{ref}}\right)^b \tag{7}$$

where the term C_{ref} is the reference cost coefficient that corresponds to a cost per unit of (one or more) physical parameter, F_{ref} and F_i are the reference and the physical variable value and b is the sizing exponent.

3.1 Solar Collector Cost Equation

The purchase cost of the solar collector (C_{solar}) is affected by two main variables: the solar collector area and the collection efficiency. The variable with the highest weight is the area (A_{solar}) [in m^2]. The collector cost equation is given by Eq. (8):

$$C_{solar} = C_{ref,\ solar} \cdot A_{ref,\ solar} \cdot \left(\frac{A_{solar}}{A_{ref,\ solar}}\right)^{b_{solar}} \cdot \left(\frac{1}{1-\eta_{collection}}\right)^c \tag{8}$$

where, the reference cost coefficient, $C_{ref,\ solar}$, is 298.54€/m^2; the reference collector area, $A_{ref,\ solar}$, is assumed to be 2.5 m^2; the area sizing factor (b_{solar}) is assumed to be

0.5, and the efficiency exponent is fixed at $c = 0.1$. The value for the collection efficiency is obtained from the Eq. (2) considering a specific climate condition.

3.2 Pump Cost Equation

The purchase cost equation of the circulation pump, (C_{pump}) is defined considering the flow rate ($\dot{V}_{pump}$) as the main operational variable affecting the cost of this component (Eq. (9)). The term $C_{ref,\ pump}$ corresponds to the constant reference cost of the pump cost, $\dot{V}_{ref,\ pump}$ [in m^3/h] is the reference pump flow rate and b_{pump} is the sizing exponent. The reference cost coefficient is equal to 322.45€/(m^3/h), the reference flow rate was assumed as 0.98 m^3/h and the sizing factor was set at 0.3.

$$C_{pump} = C_{ref,pump} \cdot \dot{V}_{ref,pump} \left(\frac{\dot{V}_{pump}}{\dot{V}_{ref,pump}} \right)^{b_{pump}} \tag{9}$$

3.3 Storage Tank Cost Equation

Regarding the storage tank cost equation, the physical variable that mostly affects its price is the storage volume ($V_{storage}$) [in m^3] as presented in Eq. (10), where the reference cost coefficient is $C_{ref,\ storage}$= 3,647.45€/m^3; the reference storage volume is assumed to be $V_{ref,\ storage}$ = 0.32 m^3; and the sizing factor is equal to $b_{storage}$ 0.3.

$$C_{storage} = C_{ref,storage} \cdot V_{ref,storage} \left(\frac{V_{storage}}{V_{ref,storage}} \right)^{b_{storage}} \tag{10}$$

3.4 Total Investment Costs

The capital investment of the components corresponds to the sum of the purchase cost of the pump cost, the storage tank cost and the solar collector cost. The estimated cost regarding the engineering expenses with the installation ($C_{installation}$) usually represents a variable percentage of the investment of the main components. Thus, the total investment costs are calculated by the Eq. (11):

$$C_{inv} = C_{pump} + C_{storage} + C_{solar} + C_{installation} + C_{circulation} \tag{11}$$

where the $C_{installation}$ was assumed to be 10% of the total cost of collector, the storage tank and the circulation pump. The circulation costs ($C_{circulation}$) were defined as a fixed value (500€), since, for the range of individual domestic applications, the prices do not vary significantly [4].

4 Optimization Modelling

Real-world optimization problems are complex to implement in terms of a number of variables, nature of the objective function or even because of the existence of many local optimal. As the one presented herein, some of the optimization problems consider more than one conflicting objective functions to be optimized, resulting in multi-objective optimization problems. A unique solution that simultaneously optimizes all the objective function does not exist and, therefore, different solutions will produce trade-offs between different objectives values. The set of solutions create a multi-dimensional function space, typically represented by Pareto curves [10].

4.1 Objective Functions, Decision Variables and Constraints

In the present study, two key objective functions were defined for optimization: the minimization of the total investment cost of the solar thermal system and the maximization of the solar collection efficiency as defined in Eq. (12):

$$\begin{aligned} &\textit{Minimize} \quad F_m(x), \qquad m = 1 \textit{ and } 2; \\ &F_1(x) = C_{inv} \\ &F_2(x) = -\eta_{collection} \end{aligned} \tag{12}$$

The definition of the decision variables is one of the most important steps in formulating an optimization problem. The variable bounds of an optimization problem restrict each decision variable to a lower and upper limit which institutes a space called decision variable space. Based on preliminary tests to the physical model, three explicit decision variables were defined in the numerical model. The selected decision variables include the maximum temperature variation that the collector can reach for certain ambient temperature and as a function of solar irradiation ($T*$), the solar collection area (A_{solar}) and the tank storage volume ($V_{storage}$). The three decision variables were lower and upper bounded as presented by the Eqs. (13), (14) and (15).

$$0.005 \leq T* \leq 0.140 \quad [^{\circ}\text{C}/(\text{W}/\text{m}^2)] \tag{13}$$

$$2.0 \leq A_{solar} \leq 8.0 \quad [\text{m}^2] \tag{14}$$

$$0.060 \leq V_{Storage} \leq 0.540 \quad [\text{m}^3] \tag{15}$$

Few linear constraints were considered regarding the significance of physical variables of the model. Table 2 identifies the linear constraints assumed in the model and depicts the reason for its consideration. These constraints aim to limit the operational parameters that give significance to the thermal model: (1) guarantee that there is a temperature difference that promotes the heat transfer between the thermal fluid and the water; (2) define the temperature limits for the thermal fluid, which is characteristically a solution of water and of propilenoglicol; (3) set a range for solar irradiation.

Table 2. Definition of linear constraints and the reason for its consideration

Linear constraint	Reason
$t_f - t_a > 10$ °C	Ensure the heat transfer process between the thermal fluid and the water
15 °C $\leq t_f \leq 180$ °C	Simple limits of thermal fluid temperature
950 W/m^2 $\leq I_g \leq 1,000$ W/m^2	Limit the solar irradiation to characteristic values for direct radiation

4.2 Optimization Algorithm: NSGA-II

In this work, a variant of NSGA-II was implemented (Fig. 3). This algorithm is a non-dominant and elitist GA that favours individuals with better fitness value (rank) and that can help to increase the diversity of the population [19]. This approach was chosen due to the convergence reduced time, the capability of solving a mathematical model with non-linear functions of a complex physical and economic model, when compared with gradient-based methods [20].

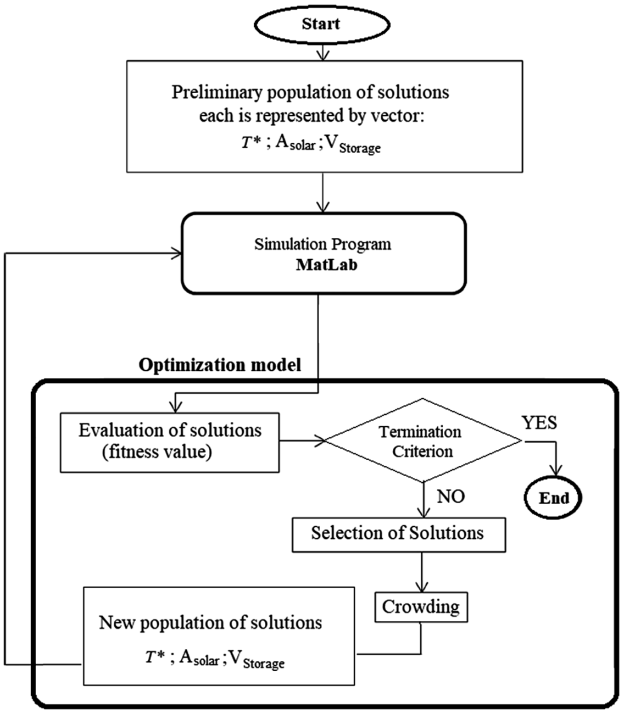

Fig. 3. Flow chart of the genetic algorithm implementation at MatLab®.

The elitist selection mechanism picks the current best solutions of each generation without applying any operators to them. However, since it uses a controlled elitist genetic algorithm, there is a balance between exploitation and exploration of the objective functions space. The algorithm creates a population that is feasible with respect to bounds and linear constraints. Each solution is denoted by the vector [T^*, A_{solar}, $V_{Storage,}$], where its elements represent the decision variables (e.g. size of the system's components). Then the algorithm evaluates the objective function and constraints for the population and it uses those values to create scores for the population through the comparison of fitness function values. The population and the offspring are combined into one matrix to extend the population, by computing the rank and crowding distance. Then, the Pareto optimal solutions are tabulated, considering that the trade-off between competing objectives is resolved. The optimization problem was solved with "*gamultiobj*" MatLab® routine, considering a population size of 60 and a Pareto fraction of 0.35. All other parameters were set according to the default values of the MatLab® routine.

5 Results and Discussion

In multi-objective optimization, each of the points in the Pareto curve represents a point where one objective function value may not be improved without worsening others. Therefore, decision-makers select one of them based on the best interest conditions. The multi-objective optimization results are expressed as a two dimensional Pareto front in Fig. 4. The optimization converged when the average change in the spread of Pareto solutions was less than the minimum distance between objective function values. The objective function was evaluated a total of 6,601 times and 109 generations were generated, minimizing the equipment purchase investment cost while the solar collection efficiency is being maximized.

As shown in Fig. 4, a set of optimal solutions for which the solar collection efficiency varies from 28.3% to 78.0% and the investment costs vary between 2,099.5€ and 3,308.3€ can be observed. From the analysis of the Pareto curve, it is shown that gains in overall efficiency above 70% imply a great increase in the total purchase cost,

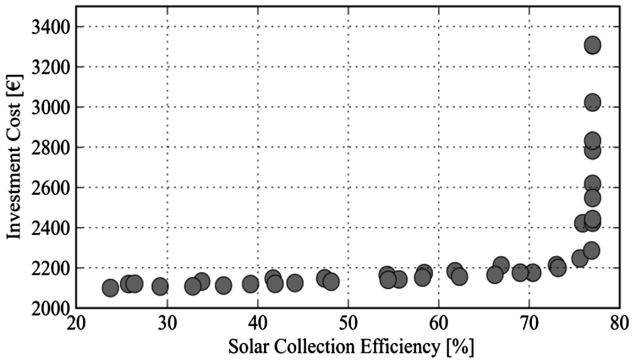

Fig. 4. Pareto optimal frontiers in objectives' solution space.

i.e., varying from a total investment cost of 2,200€ (with an efficiency of 70%) to an investment cost of 3,200€ (with an efficiency of 78%).

Table 3 presents the maximum and minimum values for the decision variables within the optimal frontiers in objectives' space. Due to the importance of the physical values such as the solar collection area and the storage volume tank in the total investment cost, both decision variables are closer to the lower bound that was considered. By the other hand, the maximum temperature that the collector can reach is affected by the solar irradiation, which has a direct and positive influence in the collection efficiency. In fact, when the fluid mean temperature is equal to the ambient temperature, the efficiency is referred as the optical one, representing its maximum value. Considering the changeability of the decision variables, a sensitivity analysis of the sizing factors in the purchase cost equations should be performed in order to better adjust the weight of the physical variables in the respective component cost.

Table 3. Maximum and minimum values for the decision variables within the optimal frontiers in objectives' solution space

Decision variable	Minimum value	Maximum value
Temperature Parameter, T^* [°C/(W/m^2)]	0.0052	0.1062
Solar Collection Area, A_{solar} [m^2]	2.032	4.260
Storage Tank Volume, $V_{storage}$ [m^3]	0.062	0.682

Figure 5 discloses a contour surface showing the variation of solar collection efficiency as a function of the solar collector area and the solar irradiation, using the optimal population results. As expected, higher solar collection areas and high values of irradiation lead to increased collection efficiencies. Thus, the sizing coefficient of the collector area in the solar collector has a great influence on problem modelling.

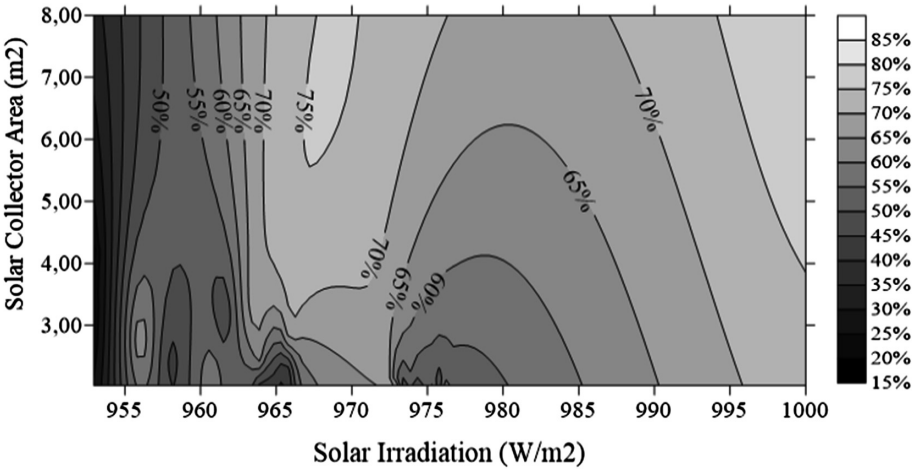

Fig. 5. Solar collection efficiency variation as a function of the solar collector area and the irradiation for the optimal solution.

Figure 6 depicts a contour surface showing the variation of the total purchase cost of the thermal system as a function of the solar collector area and the storage tank volume, using the optimal solution population results. Results a positive correlation between the increase of system cost with the solar collector area. In fact, this decision variable directly affects the sizing of all the components, and consequently the cost of all of the subcomponents.

For a combination of lower values of solar collector area and storage volumes, the variation of the total investment cost is not linear, showing that the storage volume has a greater impact on the investment.

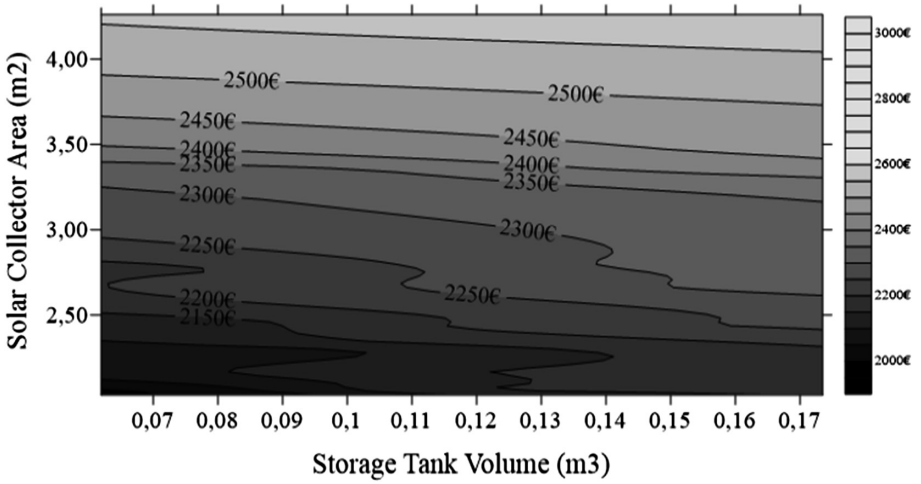

Fig. 6. Total investment cost of the thermal system as a function of the optimal solution for the solar collector area and the irradiation for the optimal solution.

6 Conclusions

In this paper, thermo-economic modelling and multi-objective optimization of a thermal solar system have been done. A multi-objective optimization was performed by defining as objective functions the maximization of solar collection efficiency and the minimization of the total purchase cost of the system. Pareto curves were obtained and analysed. According to the obtained Pareto front, the optimal solution discloses a set of function value's for which the solar collection efficiency vary 28.3% and 78.0% and the investment costs vary between 2,099.5€ and 3,308.3€. The most important decision variable is the solar collector area since this physical variable affects the sizing of the remaining subcomponents of the solar thermal system and, therefore, it deeply affects the total investment cost of the system. A sensitivity analysis of the sizing factors of the cost equations should be performed in order to improve the model accuracy in determining the relative cost of each component.

Acknowledgements. The first author would like to express her gratitude for the support given by the Portuguese Foundation for Science and Technology (FCT) through the Post-Doc Research Grant SFRH/BPD/121446/2016. This work has been supported by FCT within the Project Scope UID/CEC/00319/2019 (ALGORITMI) and Project Scope UID/EMS/04077/2019 (METRICS).

References

1. da Graça, G.C., Augusto, A., Lerer, M.M.: Solar powered net zero energy houses for southern Europe: feasibility study. Sol. Energy. **86**, 634–646 (2012). https://doi.org/10.1016/j.solener.2011.11.008
2. Neves, D., Silva, C.A.: Modeling the impact of integrating solar thermal systems and heat pumps for domestic hot water in electric systems – the case study of Corvo Island. Renew. Energy **72**, 113–124 (2014). https://doi.org/10.1016/j.renene.2014.06.046
3. Evarts, J.C., Swan, L.G.: Domestic hot water consumption estimates for solar thermal system sizing. Energy Build. **58**, 58–65 (2013). https://doi.org/10.1016/j.enbuild.2012.11.020
4. Kalogirou, S.A.: Solar thermal collectors and applications. Prog. Energy Combust. Sci. **30**, 231–295 (2004). https://doi.org/10.1016/j.pecs.2004.02.001
5. Ong, K.S., Tong, W.L.: System performance of U-Tube and heat pipe solar water heaters. J. Appl. Sci. Eng. **15**, 105–110 (2012)
6. Sahin, B., Kodal, A.: Performance analysis of an endoreversible heat engine based on a new thermoeconomic optimization criterion. Energy Convers. Manag. **42**, 1085–1093 (2001). https://doi.org/10.1016/S0196-8904(00)00120-5
7. Ferreira, A.C.M., et al.: An economic perspective on the optimisation of a small-scale cogeneration system for the Portuguese scenario. Energy **45**, 436–444 (2012). https://doi.org/10.1016/j.energy.2012.05.054
8. Ferreira, A.C., Nunes, M., Martins, L., Teixeira, S.: Maximum profit of a cogeneration system based on stirling thermodynamic cycle. In: 2014 14th International Conference on Computational Science and Its Applications, pp. 156–160. IEEE (2014)
9. Bejan, A., Tsatsaronis, G., Moran, M.: Thermal Design and Optimization. Wiley, New York (1996)
10. Assaf, J., Shabani, B.: Multi-objective sizing optimisation of a solar-thermal system integrated with a solar-hydrogen combined heat and power system, using genetic algorithm. Energy Convers. Manag. **164**, 518–532 (2018). https://doi.org/10.1016/j.enconman.2018.03.026
11. Lin, W., Ma, Z., Ren, H., Gschwander, S., Wang, S.: Multi-objective optimisation of thermal energy storage using phase change materials for solar air systems. Renew. Energy **130**, 1116–1129 (2019). https://doi.org/10.1016/j.renene.2018.08.071
12. Antoniadis, C.N., Martinopoulos, G.: Optimization of a building integrated solar thermal system with seasonal storage using TRNSYS. Renew. Energy **137**, 56–66 (2019). https://doi.org/10.1016/j.renene.2018.03.074
13. Yılmaz, İ.H.: Residential use of solar water heating in Turkey: a novel thermo-economic optimization for energy savings, cost benefit and ecology. J. Clean. Prod. **204**, 511–524 (2018). https://doi.org/10.1016/j.jclepro.2018.09.060
14. Asadi, J., Amani, P., Amani, M., Kasaeian, A., Bahiraei, M.: Thermo-economic analysis and multi-objective optimization of absorption cooling system driven by various solar collectors. Energy Convers. Manag. **173**, 715–727 (2018). https://doi.org/10.1016/j.enconman.2018.08.013

15. Tian, Y., Zhao, C.Y.: A review of solar collectors and thermal energy storage in solar thermal applications. Appl. Energy **104**, 538–553 (2013). https://doi.org/10.1016/j.apenergy.2012.11.051
16. Lebeña, E.P., Costa, J.C.: Installers of thermal solar equipment. In: INETI/DGEG (ed.) Conversão Térmica da Energia Solar, pp. 1–89. INETI/DGEG, Lisboa (2008)
17. Greenstream Publishing: Solar Electricity Handbook. http://www.solarelectricityhandbook.com/solar-irradiance.html
18. Ferreira, A.C., Nunes, M.L., Teixeira, J.C.F., Martins, L.A.S.B., Teixeira, S.F.C.F.: Thermodynamic and economic optimization of a solar-powered Stirling engine for micro-cogeneration purposes. Energy **111**, 1–17 (2016). https://doi.org/10.1016/j.energy.2016.05.091
19. MathWorks, M.: gaoptimset: Create genetic algorithm options structure (2014). https://www.mathworks.com/help/gads/gamultiobj.html
20. Ferreira, A.C.M., Rocha, A.M.A.C., Teixeira, S.F.C.F., Nunes, M.L., Martins, L.B.: On solving the profit maximization of small cogeneration systems. In: Murgante, B., et al. (eds.) ICCSA 2012. LNCS, vol. 7335, pp. 147–158. Springer, Heidelberg (2012). https://doi.org/10.1007/978-3-642-31137-6_11